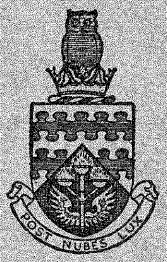

THE COLLEGE OF AERONAUTICS

CRANFIELD

AN EXPERIMENTAL METHOD OF DETERMINING THE MEAN HEAT TRANSFER COEFFICIENT FOR THE NOZZLE OF A SOLID PROPELLANT ROCKET ENGINE, BY MEANS OF CONSTANT FLOW CALORIMETRY

by

A. G. Smith and T. A. Carberry

NOTE NO. 122

January, 1962.

THE COLLEGE OF AERONAUTICS

CRANFIELD

An Experimental Method of Determining the Mean Heat Transfer Coefficient for the Nozzle of a Solid Propellant Rocket Engine, by means of Constant Flow Calorimetry

- by -

A. G. Smith,* B.Sc., A.R.C.S., D.I.C., A.F.R.Ae.S.,

and

T. A. Carberry, A.F.Inst.Pet.

SUMMARY

An investigation has been made into the feasibility of predicting mean convective heat transfer coefficients for the nozzles of solid propellant rocket engines. The principle of the method used was constant flow calorimetry; the surface of a copper nozzle was heated with a flow of hot water, and cooled by air flow through the nozzle. Heat transfer coefficients were then derived from measurements of water flow, water temperature drop and nozzle surface temperatures. For a range of Reynolds numbers, the mean convective heat transfer for a star-shaped conduit could be expressed by the following equation:-

$$Nu = 0.1976\ Re^{0.631}\ Pr^{0.333}$$

For a cigarette-burning charge the mean convective heat transfer could be expressed by the following equation :-

$$Nu = 0.7013\ Re^{0.491}\ Pr^{0.333}$$

The flow pattern into the nozzle was studied using a water flow visualisation rig involving both photographic and direct viewing techniques. In addition, investigations into the temperature and pressure distributions along the nozzle surface at ambient conditions were carried out using a perspex nozzle fitted with surface thermocouples and pressure tappings.

---

* Hives Professor and Head of Department of Mechanical Engineering, University of Nottingham.
Formerly Professor and Head of Department of Aircraft Propulsion, The College of Aeronautics.

CONTENTS

NOTATION

A_s	surface area of nozzle, ft^2
A_T	throat area of nozzle, ft^2
C_{p_w}	specific heat of water at constant pressure cal./grm.C^o.
D_T	throat diameter of nozzle, ft.
$\bar{h}$	average heat transfer coefficient. C.H.U./hr.ft^2.C^o.
$\bar{h}_L$	coefficient of heat leakage to surroundings. C.H.U./hr.ft^2.C^o.
$\bar{h}_o$	observed average heat transfer coefficient. C.H.U./hr.ft^2.C^o.
Δh	differential head across metering orifice. ins. water gauge.
K	thermal conductivity of air. C.H.U./hr.ft.C^o.
Nu	Nusselt Number $\left(\frac{h D_T}{K}\right)$
p	pressure of air at upstream tapping of orifice. "Hg. gauge.
P_a	atmospheric pressure. "Hg.
Re	Reynolds Number $\left(\frac{W D_T}{\mu A_T}\right)$
T_a	air temperature upstream of orifice. ^oC.
T_s	surface temperature of nozzle. ^oC.
T_{w_1}	temperature of water at inlet to nozzle. ^oC.
T_{w_2}	temperature of water at outlet from nozzle. ^oC.
ΔT_w	temperature drop of water through nozzle. C^o.
V_w	volume flow rate of water. cm^3/sec.
W	air mass flow rate. lb./sec.
ϵ	expansion coefficient
μ	absolute viscosity of air. lb./hr.ft.
ρ_w	density of water. grm./cm^3.

1. Introduction

The temperature of a rocket engine nozzle is often a design limitation. In order to determine this temperature, a knowledge of the coefficient of heat transfer by convection from the gas to the surface is required.

It has been noted that conditions upstream of the nozzle, e.g. the geometry of the conduit of a solid propellant engine, influence the rate of heat transfer to the nozzle. In the case of star-shaped solid propellant charges, there is a tendency for the converging (upstream) surface of the nozzle to be eroded, thus affecting the performance of the engine. This tendency is more marked with hot propellants than with cool; however, it has been noted also that with cigarette-burning charges the erosion of this nozzle region is often much less marked.

Certain obvious hypotheses arise: clearly when the jet issuing from a star-shaped conduit strikes the nozzle entry face, conditions are obviously favourable to the existence of marked secondary flows. In fact, each stream from a star point of the conduit would be expected to impinge obliquely on the nozzle entry face and then splash sideways, with consequent continued renewal of the hot stream on the nozzle surface, hence giving rise to high heat transfer, friction, and erosion.

In the case of the cigarette-burning charge, there would be no jet impingement action, no secondary flow, less friction and heat transfer, and less tendency to erosion.

Experiments on nozzle erosion could not be undertaken at Cranfield owing to the expense of the rockets and the requisite labour. However, investigations of heat transfer coefficients by convection, both local and mean, have been carried out. Local heat transfer coefficients were obtained by Lt. R.M.Houston (Ref.1) and Flt.Lt. I. Singh (Ref. 2), using a mass transfer method involving napthalene. The investigation of mean heat transfer coefficients by convection is dealt with in this report.

Conduit Design

The rocket motor casing was manufactured from a perspex tube 4.5" internal diameter and 18" long. Perspex grain models of any conduit design could be slid into this tube and secured firmly in the required axial position relative to the nozzle. To obtain a highly disturbed flow pattern at the nozzle, a seven-pointed star shape conduit with a low value of conduit cross-section to throat area ratio was chosen.

Using Stone (Ref. 3) as a guide, a seven point star conduit was designed with the following characteristics :-

(a) Progressivity ratio

$$= \frac{\text{final propellant surface}}{\text{initial propellant surface}} = 1.0$$

(b) Loading fraction

$$= \frac{\text{propellant cross section}}{\text{motor cross section}} = 0.75$$

which when used in conjunction with a nozzle of 1.98" throat diameter, resulted in a conduit cross section to throat area ratio of 1.3, as recommended by R.P.E., Westcott.

The conduit model featured perspex flanges at each end and another midway along its length. The star shape was made from 1/16" thick perspex sheet, each point being folded separately to the required radius and then bonded to other points and to the locating flanges. The complete model was 16" long (Fig.10).

Nozzle Design

The nozzle shape was produced to R.P.E. Westcott recommendations, the converging face being a cone of half angle of 60° turned into the throat by an arc of a circle whose radius was equal to the throat radius. The throat area was approximately 0.77 of the conduit area, thus giving a throat diameter of 1.98". The diverging face, when incorporated for the flow visualisation studies and for the mass transfer investigations, had an included angle of 30°.

2. Mean Heat Transfer Determination

Apparatus

The principle of the method used was constant flow calorimetry. The surface of a copper nozzle was heated by a flow of hot water and cooled by air flow through the nozzle. Rates of heat transfer were derived from measurements of flow and temperature drop of the water. Nozzle surface temperatures were also measured and hence the heat transfer coefficients calculated.

The apparatus is shown diagrammatically in Fig. 3. The water in the main tank (which was well insulated to reduce heat leakage to a minimum) was heated by four 2.KW. immersion heaters, one of which was controlled by a Variac, so that the water temperature at inlet to the nozzle could be maintained reasonably constant. The water was pumped round the system by means of an electrically driven centrifugal pump and the water volume flow rate determined from a visual reading flowmeter.

The airflow was supplied from an Allis Chalmers compressor, the air being drawn through the conduit and nozzle and thence through a metering orifice. The installation was on the suction side of the compressor for the following reasons :-

(a) The danger of velocity and temperature tratification of the air flow was thereby considerably reduced.

(b) Measurement of air flow total temperature (i.e. ambient air temperature) was simplified.

(c) The rig components (e.g. perspex models, etc.) were not subjected to more than 15 lb./in^2 pressure.

(d) Control of flow down to very low values could be achieved by altering the compressor suction butterfly valves without introducing turbulence into the working section.

To determine the heat transfer from the surface of the nozzle to the air, hot water at approximately 85°C. was circulated through the passageways in the nozzle. The temperature drop of the water flowing through the nozzle was determined by means of a chromel-constantan differential thermocouple connected to a galvanometer. The actual water temperatures at inlet and outlet to the nozzle were measured with mercury-in-glass thermometers (range 55-105°C. x 0.2 C°), these thermometers all having an N.P.L. certificate. The nozzle surface temperature was obtained from the mean reading of six copper-constantan thermocoaxial thermocouples embedded in the wall of the nozzle.

Tests were carried out over a range of air flows from 500 lb./hr. to approximately 3200 lb./hr. (i.e. choking conditions in nozzle), using (a) the star-shaped conduit configuration, and (b) the cigarette-burning shaped configuration. In addition, the distance of the conduit to the nozzle entry face was varied from zero to 0.75".

3. Nozzle Construction

The nozzle was manufactured from solid copper bar, copper being chosen for its excellent thermal characteristics. The production of the passageways presented some problems, ideally a spiral form was envisaged, but due to the nozzle profile it seemed that to produce this form would be too costly. The finalised form was a series of concentric grooves 0.125" wide by 0.1875" deep. A slot was cut in each separating wall between the grooves to allow the water to flow from one groove to the next, each groove being suitably blanked off to form a continuous passageway approximately 65" long. Six copper-constantan thermocoaxial thermocouples of 0.02" diameter were embedded in the nozzle surface at random positions, the nozzle surface being of the order of 0.062" thick. The outside of the grooves was then sealed off by means of copper strips soldered on to the top of the separating walls. The nozzle was sandwiched between two 0.625" thick ebonite flanges, and the intervening space filled with powdered asbestos to reduce all heat losses, other than the heat lost to the air flow, to a minimum (Fig. 11).

The maximum water flow rate through the passageways was 1625 cc./min. at a pressure of 30 p.s.i.g. The weight of the copper nozzle was 1.26 lb., and the calculated temperature drop across the wall was of the order of 0.05°C. maximum.

4. Temperature Measurement

Calibration of the Chromel-Constantan Differential Thermocouple

Since the temperature drop of the water flowing through the nozzle was always small, it was essential that the measurement of various temperatures required from the apparatus should be accurately obtained. All temperature measuring instruments were therefore carefully calibrated.

In the case of the chromel-constantan differential thermocouple, the ends of the thermocouple were placed in separate oil baths (thermos flasks) each containing an electrically driven stirrer, a small heating element, and an N.P.L. calibrated mercury-in-glass thermometer (range 55-105°C. x 0.2 C°). The ends of the leads were connected via a cold junction to a spot galvanometer. Oil was heated to about 85-90°C. and poured into the oil baths; one oil bath had a small quantity of cold oil added until the temperature difference betwen the two baths was about 4 C°. By means of rheostats and ammeters, incorporated in the heating coil circuits, it was possible to maintain a constant temperature difference between the two oil baths. The galvanometer deflection was calibrated against a Beckmann differential thermometer (range 6 C° x 0.01 C°), and a suitable calibration curve was produced.

Stratification in Main Supply Tank

To check on the effect of temperature drift arising from stratification of the water in the heating tank, a temperature drift indicator was made. This consisted of a 0.25" bore copper tube approximately 61" long, made into a coil of 3.75" diameter and having 5 turns, the whole weighing 1.25 lb., sensibly the same as the copper nozzle. Two constantan wires were soldered one at each end of the coil, and the ends of the qires were connected to a spot galvanometer via a cold junction. The coil was well insulated with mineral wool inside an aluminium container 6" x 6" x 3" in size, and was placed in the supply line between the pump and the nozzle. The sensitivity of the galvanometer was such that one centimetre deflection on the scale was equivalent to 0.6 C°. It was found, for the range of tests covered, that the instrument was quite sensitive to sudden changes in temperature, and no significant changes in temperatures due to stratification were observed once steady state conditions had been achieved.

5. Heat Leakage

It was necessary to determine the amount of heat leakage from the nozzle, other than that through the nozzle surface. To obtain this factor, the conduit and motor case were removed from the nozzle, and the nozzle surface completely insulated from the atmosphere with cotton wool. Hot water at the normal working temperature was circulated through the nozzle passageways, starting at the maximum water flow rate and gradually reducing the flow rate in stages to the minimum likely to be used. Values of heat leakage were determined at each of these stages after steady state conditions had been established. These values have been plotted in graphical form (Graph 3).

6. Treatment of Results

Air Flow Measurement

1. The air mass flow rates were measured using British Standard orifice plates with D and D/2 pressure tappings. Using Ref. 4, it was calculated that two orifice plates would be sufficient to cover the range of flows from 300 to 3600 lb./hr. The mass flow equations are :-

(a) 3.8" dia. orifice plate

$$W \text{ lb./sec.} = 0.825\ \epsilon \sqrt{\frac{P.\ \Delta h}{T_a}}$$

(b) 1.9" dia. orifice plate

$$W \text{ lb./sec.} = 0.186\ \epsilon \sqrt{\frac{P.\Delta h}{T_a}}$$

where P = pressure upstream of orifice "hg. abs.

Δh = differential head across orifice plate "water gauge

T_a = temperature of air upstream of orifice ^{o}K.

ϵ = expansion coefficient

Since the total temperature of the air flow was atmospheric temperature, readings were taken from a mercury-in-glass thermometer (range -5 to 55^{o}C. x 0.2 C^{o}) placed at the conduit entrance.

2. Water Volume Flow Rate

$$V_{w_2} \text{ cc/sec.} = \frac{\text{flowmeter reading} \times V_{w_{max}} \sqrt{\frac{\rho_{w_{20}}}{\rho_{w_2}}}}{60}$$

$$= \text{flowmeter reading} \times 37.88 \sqrt{\frac{\rho_{w_{20}}}{\rho_{w_2}}}$$

where $V_{w_{max}}$ = water volume flow rate at full scale meter reading at 20^{o}C
= 2273 cc/min.

$\rho_{w_{20}}$ = water density at 20^{o}C.
= 0.998 grm/cc.

ρ_{w_2} = water density at T_{w_2} (Graph 2)

T_{w_2} = water outlet temperature from nozzle ^{o}C.

Values of water density over range of temperatures were obtained from Kaye and Laby (Ref. 5).

3. The values of absolute viscosity of air, and thermal conductivity of air were obtained from Kays and London (Ref. 6).

Theory

If hot water is circulated around the copper nozzle when air is passing through the nozzle, then the heat lost by the water can be equated to the heat gained by the air. Hence the mean value of the heat transfer of the nozzle by convection can be determined.

Heat transferred = $(\rho.V.C_p\ \Delta T)_w$ grm. cal./sec.

$$q'' = \bar{h}_o A_s (T_s - T_a) \text{ CHU/hr.}$$

$$\therefore \quad \bar{h}_o = \frac{(\rho.V.C_p.\Delta T)_w \times 7.938}{A_s (T_s - T_a)} \quad \text{CHU/hr.ft}^2\ C^{o}.$$

where A_s = surface area of nozzle = 0.1241 ft^2

C_{p_w} = specific heat of water at T_{w_2} grm. cal./grm. C^o (Graph 2)

ρ_w = density of water at T_{w_2} grm./cc. (Graph 2)

T_{w_2} = water outlet temperature from nozzle ^oC.

T_s = mean surface temperature of nozzle ^oC.

T_a = air temperature ^oC.

7.938 = conversion factor to convert grm. cal./sec. to CHU/hr.

Values of C_{p_w} were obtained from reference 5.

Heat leakage $\bar{h}_L$ to surroundings, over the range of flows covered in the tests, was obtained from (Graph 3).

$\therefore$ $\bar{h} = \bar{h}_o - \bar{h}_L$ CHU/hr.ft^2 C^o.

Now the Nusselt No. $Nu = \dfrac{\bar{h} D_T}{K}$

where D_T = nozzle throat diameter = 0.165 ft.

K = thermal conductivity of air CHU/hr.ft.C^o.

The Reynolds No. $Re = \dfrac{W}{\mu} \dfrac{D_T}{A_T} \times 3600 = 2.76 \times 10^4 \, W/\mu$

where W = air mass flow rate lb./sec.

D_T = nozzle throat diameter = 0.165 ft.

A_T = nozzle throat area = 0.0215 ft^2.

μ = absolute viscosity of air lb./hr.ft.C^o.

The results of the test carried out have been plotted in the form of Nu against Re and are shown (Graph 1). A value of 0.71 was taken for the Prandtl No. and hence the following relationships were derived from the plotted results.

For the case of the star-shaped charge :

$$Nu = 0.1976 \, Re^{0.631} \, Pr^{0.333}$$

and the case of the cigarette burning charge

$$Nu = 0.7013 \, Re^{0.491} \, Pr^{0.333}$$

7. Flow Visualisation

To be able to assess the variations of nozzle heat transfer coefficient in relation to the air flow pattern, it was considered desirable to be able to visualise and study this pattern.

A three dimensional water flow visualisation rig was constructed (Fig. 6), and basically consisted of models of rocket components made of perspex, identical in size to those used in the heat transfer apparatus. Water was pumped by means of a small centrifugal pump through the models and recirculated back to the storage tank. Flow and pressure control were achieved by suitable valves and a British Standard orifice plate was used to determine the water mass flow rate. The flow tracers used were polystyrene pellets of the order of 0.3 - 0.5 mm. diameter and having a density close to that of water.

The light source used for general viewing was 3 KW line filament tungsten lamp; an adjustable slit on the side of the lamp running parallel to the filament concentrated the light into the required beam. The lighting source could be moved bodily so that various cross-sections of the flow conditions could be studied.

The star-shaped conduit model was specifically designed with seven points so that by passing a beam of light directly across the diameter of the model it was possible to view, simultaneously the flow patterns issuing from a peak of the star-shape, and also the flow patterns issuing midway between two peaks. To provide permanent records of the flow patterns, photographs were taken by Houston (Ref. 1) using (a) a 120 mm. plate camera loaded with Royal x Pan film with an exposure time of 1/25 sec. at f 4.5, and (b) a 35 mm. camera using HP3 film, exposure time 1/25 sec. at f 2.8. Full illumination from the 3 KW tungsten lamp was used. The flow patterns in Figs. 7 - 9 clearly indicate the unsteady and recirculating flow issuing from the peaks of the star-shaped conduit.

8. Surface Temperature Measurement

The final stage of the investigation was to determine the adiabatic wall temperature distribution along the surface of the nozzle under ambient conditions, and to a lesser degree the static pressure distribution. For this work the nozzle was made from solid perspex bar, the convergent section only being used. Seven static pressure tappings were drilled normal to the surface of the nozzle, and at equal spacings along the nozzle surface in a horizontal plane. Diametrically opposite were installed seven chromel-constantan thermocouples made from 0.005" diameter wire: these were embedded in the surface of the nozzle by laying them in grooves 0.008" deep and sealing with perspex cement; the whole surface was then repolished to remove irregularities (Fig. 11).

Provision was made for rotating the conduit in relation to the pressure and temperature tappings, by placing 0.1875" diameter steel ball bearings in the grooves machined in the end flanges of the conduit model, formerly used for the friction rings in the flow visualisation apparatus. A degree marker was fitted to the outer flange of the perspex motor case, so that the conduit could be moved to any given position in relation to the tappings in the nozzle. The conduit model was the same as that used in previous tests, and the profile of the perspex nozzle was made to the same speicifications as the other nozzles used in these investigations. The nozzle and conduit model were connected to the same air supply as was used for the heat transfer apparatus (Fig. 2).

Tests were carried out at choking conditions in the nozzle, with the star-shaped conduit in position, and with it removed. At first, tests were carried out taking pressures and temperatures for complete rotation of the conduit, but results showed that it was only necessary to carry out further tests at two

positions: (a) when the peak of the star was in line with the tappings, and (b) when the peak was not in line (i.e. a rotation of 25.7°). The star-shaped conduit was also moved in stages from being in contact with the nozzle entry face to 0.75" from the nozzle face; no significant variation in readings was noted.

Results were plotted graphically in the form of $\frac{T_t - T_s}{T_t}$ and $\frac{P_t - P}{P_t}$

where T_t = total temperature °K

T_s = nozzle surface temperature °K

P_t = total pressure "Hg.abs.

P = nozzle static pressure "Hg.abs.

Instrumentation

All pressures were measured from 40" mercury manometers; the surface thermocouples were connected differentially with a chromel-constantan thermocouple sited in the air stream at entrance to the motor casing. The entry air temperature was measured independently with a chromel-constantan thermocouple and also with an N.P.L. calibrated thermometer (range -5 to 55°C. x 0.2 C°.). A potentiometer was used to measure the e.m.f's generated by the thermocouples. Air flow measurements were carried out as described earlier in this report.

9. Discussion

Much of the puboished heat transfer data for rocket nozzles seems to be confined to liquid propellant rocket engines, where there is relatively smooth axisymmetric flow from the combustion chamber to the nozzle. With the solid propellant engine, the geometry of the charge markedly influences the flow conditions at entry to the nozzle, with the result that a solid propellant charge having excellent burning characteristics may have to have its conduit shape modified to prevent serious erosion of the convergent face of the nozzle.

The experimental method in this report suggests a practical and relatively straightforward way of examining the effect of different conduit shapes on the mean convective heat transfer coefficients of a nozzle. While the test rig does not simulate combustion, it does have the advantage that the effective diameter of the conduit remains constant throughout the test, so that investigations can be carried out at the worst flow conditions, (i.e. commencement of burning in the actual case when the velocity of the gases are at their peak) for as long as is felt necessary.

For turbulent flow conditions Wimpress (Ref. 7) suggests a relationship of $Nu_D = 0.023\ Re_D^{0.8}\ Pr^{0.4}$, (where D is the effective diameter of the flow channel), which is the generally accepted formula for fully developed turbulent flow in pipes with length/diameter ratios ≥ 4.0. Entry conditions to a nozzle have an important effect on the boundary layer conditions, and in the case of the star-shaped conduit used in these investigations, the results (Graph 1) suggest a mixture of laminar and turbulent boundary layer. The relationship obtained $Nu = 0.1976\ Re^{0.63}\ Pr^{1/3}$ is similar to that of Winding and Cheney (Ref. 8)

for tubes in cross flow.

It was found that the variation of the distance between the conduit and the nozzle entry face (i.e. 0 - 0.75") had no significant effect on the mean heat transfer coefficient.

The disturbed conditions at entry to the nozzle are clearly shown in Figs. 7 - 9 obtained from the flow visualisation apparatus. The main flow out of the conduit appears to maintain its star-shape (Fig. 7) but the secondary flow outside of this region is a combination of two vortex systems (Fig. 9), giving strong reverse fluid flow and causing a vigorous scouring action on the nozzle surface. This action must, in the case of actual combustion, lead to high local heat transfer coefficients and, ultimately, erosion of the nozzle. Houston (Ref. 1) found that these high local heat transfer coefficients occurred opposite the star outer points, as was expected and also between the star points closer to the nozzle throat. They are probably caused by the turbulent interaction of the vortex pairs. Work carried out by Singh (Ref. 2) using the mass transfer technique for determining local heat transfer coefficients, shows good agreement with the mean values obtained with the star-shaped conduit.

A calculation was carried out using the dimensions of the test nozzle to determine the mean heat transfer coefficients in a laminar boundary with constant fluid properties and a constant surface temperature. The method used was that outlined by Smith and Spalding (Ref. 9). The results are shown plotted on Graph 1 and in tabular form.

10. Conclusions

The constant flow calorimetry apparatus described in this report, together with the flow visualisation apparatus and the mass transfer technique, can provide valuable information on the variation of the mean and local heat transfer coefficients of nozzles due to the variation of the conduit shapes of solid propellant charges.

Repeatability was an essential feature of this work, and the number of tests carried out with such small scatter gives considerable confidence in the results obtained.

It is felt that further work should be carried out with this type of apparatus, using different conduit shapes and different nozzle profiles, as it is not possible to determine accurately these heat transfer coefficients from theoretical predictions alone.

11. References

1. Houston, R.M. — Nozzle heat transfer predictions from sublimation measurements on a model of a solid fuel rocket. College of Aeronautics Thesis, June, 1960.

2. Singh, U. — Nozzle heat transfer predictions from sublimation measurements on a model of a solid fuel rocket. College of Aeronautics Thesis, June, 1961.

3. Stone, M.W. — A practical mathematical approach to grain design. Jet Propulsion, vol.28, 1959, pp 236-244.

4. Flow measurement. British Standards Institution, B.S.1042, 1943.

5. Kaye, G.W.C., Laby, T.H. — Physical and Chemical Constants. 1948. Longmans Green & Co.

6. Kays, W.M., London, A.L. — Compact heat exchangers. The National Press, Palo Alto, California.

7. Wimpress, R.N. — Internal ballistics of solid fuel rockets. 1950. McGraw Hill Book Co. Inc.

8. Winding, C.C., Cheney, A.J. — Mass and heat transfer in tube banks. Ind. and Engg. Chem. vol.40, 1948, pp 1087-1093.

9. Smith, A.G., Spalding, D.B. — Heat transfer in laminar boundary layer with constant fluid properties and constant wall temperature. Roy. Aero. Soc. vol.62, 1958, pp 60-66.

10. Eckert, E.R.G. — Die Berechnung des Warmeubergangs in den laminaren Grenzschicht umstromter Korper. Z. Ver. dtsch. Ing. Forschungsheft, 4.6, 1942.

11. Mangler, W. — Zusammenhang zwischen ebenen und rotationssymmetrischen Grenzschichten in kompressiblen Flussigkeiten. A. angew. Math. Mech. vol.28, 1948.

Notation to Appendix 1

A	number defined in equation (1)
B	number defined in equation (1)
c	characteristic length of body, i.e. throat diameter of nozzle.
Δ_4	"heat flux thickness" defined by $h = k/\Delta_4$
h_m	mean heat transfer coefficient
h	heat transfer coefficient
k	thermal conductivity of the fluid
Nu	Nusselt No. (hc/k) (local)
Nu_m	Nusselt No. $(h_m c/k)$ (mean)
ν	kinematic viscosity of the fluid
Re	Reynolds No. $(U\ c/\nu)$
U	approach or reference velocity, i.e. velocity at the throat of nozzle
U_1	mainstream velocity at a point on the surface, i.e. velocity at x
x	distance along surface of nozzle
y	distance normal to surface
$\bar{}$	bar represents two dimensional flow

APPENDIX 1

Theoretical Calculation of the Heat Transfer Coefficients for Laminar Flow through the Nozzle Configuration used in the Experimental Work

Numerous approximate methods are available to calculate heat transfer in a laminar boundary layer with constant fluid properties and constant wall temperature. The simplest of all the methods appears to be that of Smith and Spalding (Ref. 9) whose simple quadratures give results identical with those of Eckert (Ref. 10).

Therefore, the theoretical calculations using dimensions of the experimental nozzle, and the velocity profile from (Graph 5) were carried out by the method of Smith and Spalding. Their equations in a simple form are :-

$$\left(\frac{\Delta_4}{c}\right)^2 \left(\frac{U\,c}{\nu}\right) = \frac{A}{\left(\frac{U_1}{U}\right)^B} \int_0^{x/c} \left(\frac{U_1}{U}\right)^{B-1} \cdot d\left(\frac{x}{c}\right) \qquad (1)$$

and

$$\frac{h\,c}{k} \Big/ \sqrt{\frac{U\,c}{\nu}} = \frac{1}{\left(\frac{\Delta_4}{c}\right)\sqrt{\frac{U\,c}{\nu}}} \qquad (2)$$

the values of A and B for Pr = 0.70 are: A = 11.68, B = 2.87.

The above mentioned equations are valid only for two dimensional flow. To obtain results for the nozzle, all the dimensions were converted to the corresponding two dimensional units by the use of the following Mangler's transformations (Ref. 11).

$$\bar{x} = \int_0^x \frac{r^2}{c^2}\,dx \qquad \bar{y} = (r/c)\,y$$

$$\bar{\Delta} = (r/c)\,\Delta \qquad \bar{h} = (c/r)\,h$$

$$\bar{U} = U$$

The mean heat transfer coefficient was obtained by :-

$$h_m = \frac{\int h.r.dx}{\int r.dx}$$

or

$$\frac{h_m c}{k} \Big/ \sqrt{\frac{U\,c}{\nu}} = \frac{\int \left(\frac{hc}{k}\right) \Big/ \sqrt{\frac{U\,c}{\nu}} \cdot \frac{r}{c} \cdot dx}{\int \left(r/c\right) dx}$$

The above integrations were carried out by the use of Simpson's Rule. Values of local heat transfer coefficients for equal intervals of x/c were obtained from (Graph 6).

The mean heat transfer coefficient obtained using the experimental nozzle dimensions is :-

$$Nu_m / \sqrt{Re} = 0.395$$

or $$Nu_m = 0.395 \ Re^{0.5} \text{ for } Pr = 0.70$$

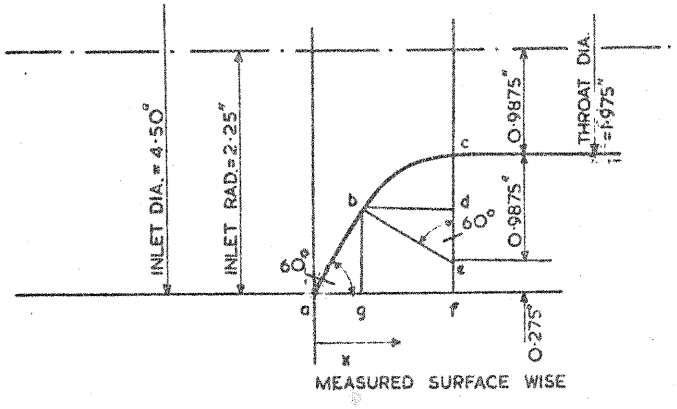

DIMENSIONS NOT SHOWN ON DIAGRAM

ab = 0·8877"
bg = 0·7687"
ed = 0·4937"

GEOMETRY OF NOZZLE.

RESULTS

$\bar{x}/c$	x/c	$\bar{U}_1/\bar{U}$	I	11.68 I	$\frac{11.68\ I}{(\bar{U}_1/\bar{U})^{2.87}}$	$\bar{Nu}/\sqrt{\bar{Re}}$	$Nu/\sqrt{Re}$
0	0	0.10	0	0	∞	∞	∞
0.05	0.0418	0.105	0.00070	0.00818	6.312	0.3981	0.4405
0.10	0.0845	0.115	0.0015	0.0175	8.536	0.3423	0.355
0.15	0.1316	0.130	0.00248	0.290	10.10	0.3147	0.323
0.20	0.1797	0.145	0.00371	0.0433	11.04	0.3010	0.297
0.25	0.2319	0.163	0.00451	0.0527	9.616	0.3225	0.3025
0.30	0.2916	0.190	0.00566	0.0661	7.74	0.3594	0.317
0.35	0.3620	0.230	0.00737	0.0861	5.817	0.4146	0.342
0.40	0.4370	0.281	0.010	0.1168	4.431	0.4751	0.351
0.45	0.5190	0.352	0.0143	0.1670	3.340	0.5472	0.379
0.50	0.6116	0.450	0.0214	0.250	2.470	0.6361	0.399
0.55	0.7276	0.590	0.0333	0.390	1.773	0.7514	0.431
0.60	0.8840	0.825	0.0550	0.642	1.114	0.9434	0.478
0.625	1.0	1.0	0.0762	0.890	0.890	1.06	0.53

$$I = \int_0^{\bar{x}/c} (\bar{U}_1/\bar{U})^{1.87}\ d\left(\frac{\bar{x}}{c}\right) \qquad \bar{Nu}/\sqrt{\bar{Re}} = \frac{\bar{h}c}{k} \Big/ \sqrt{\frac{\bar{U}c}{\nu}}$$

GRAPH. 1.

A & B Experimental Results

A. Charge before nozzle

$Nu = 0.1976\ Re^{0.631}\ Pr^{1/3}$

B. Charge removed.

$Nu = 0.7013\ Re^{0.491}\ Pr^{1/3}$

C. $Nu = 0.023\ Re^{0.8}\ Pr^{0.4}$

D. Theoretical result for axisymmetric laminar flow

$Nu = 0.395\ Re^{0.5}$ for $Pr = 0.70$

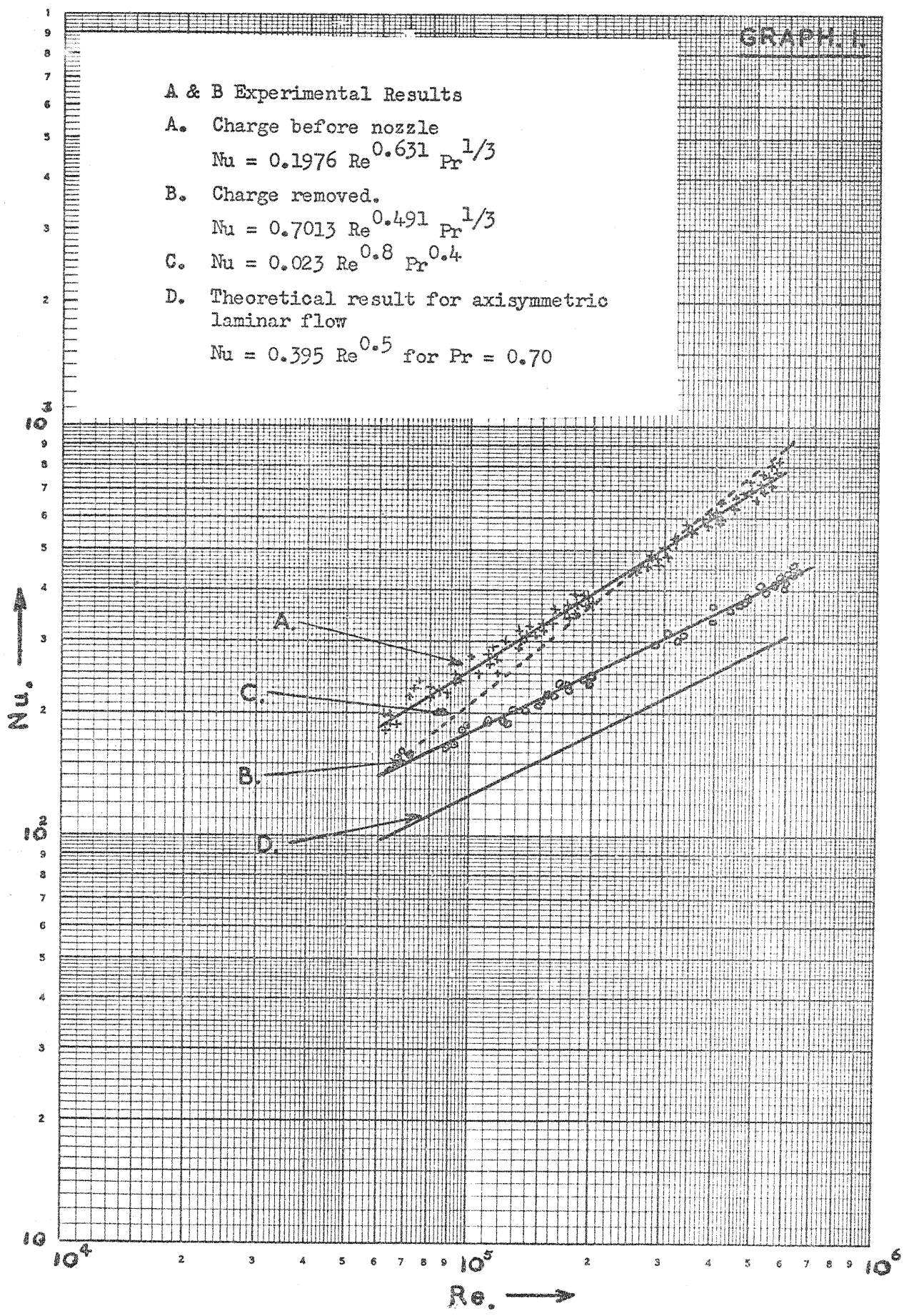

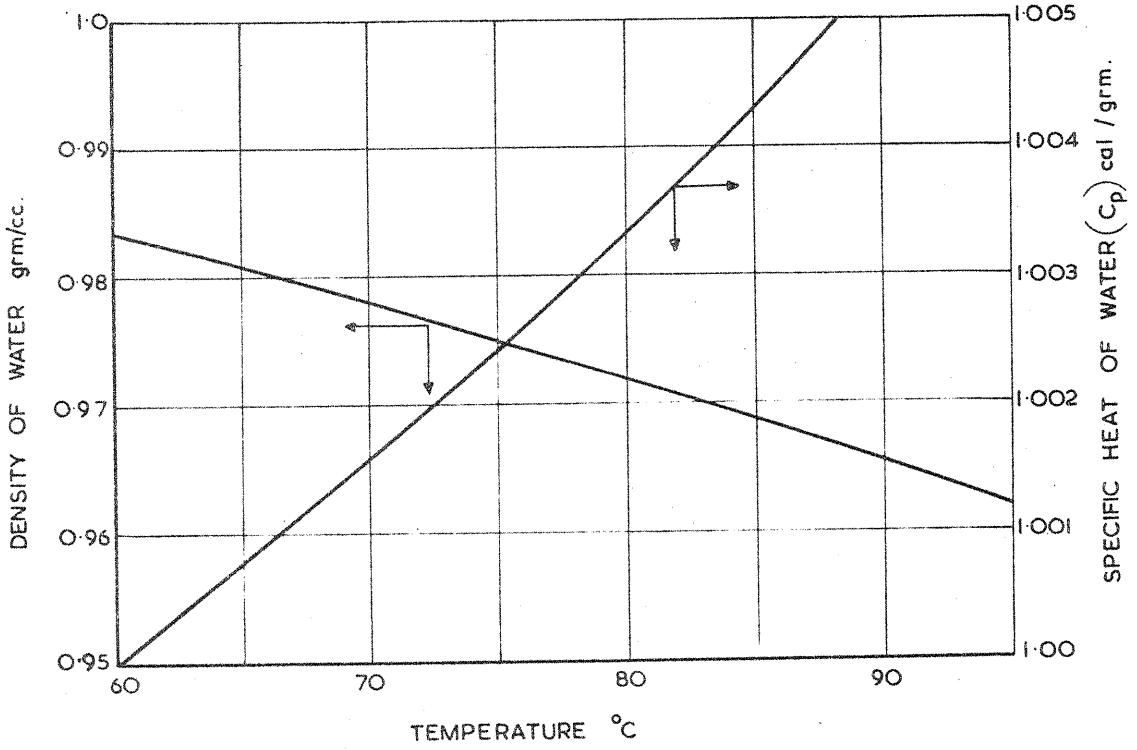

GRAPH. 2.

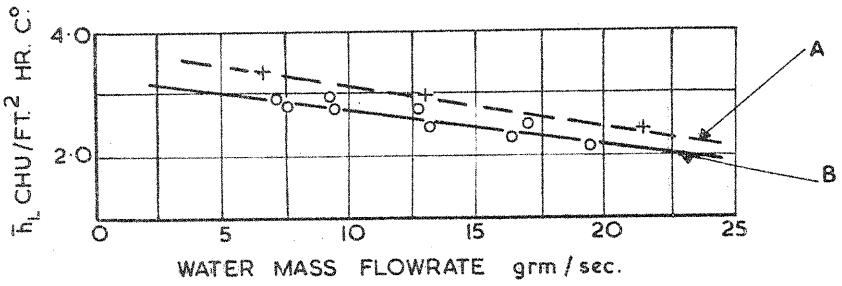

A. 1 HR. SETTLING TIME FOR EACH POINT.
B. 10 MINS " " " "

(NOTE $\bar{h}_L$ SHOULD BE CONSTANT, HOWEVER VARIATION IS VERY SMALL.)

GRAPH. 3a. HEAT LEAKAGE. v WATER MASS FLOWRATE. NOZZLE FACE INSULATED. NO AIRFLOW.

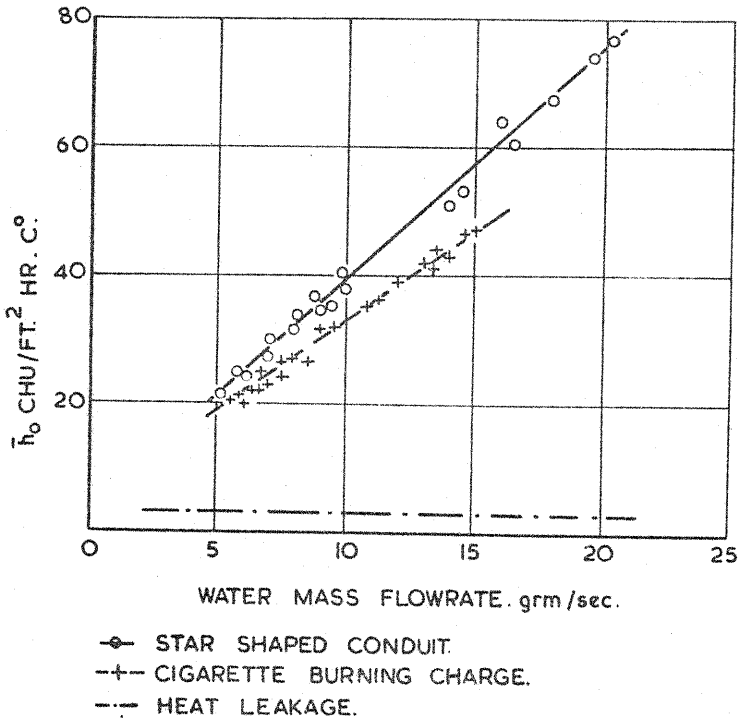

GRAPH. 3b. HEAT FLOWRATE v WATER MASS FLOWRATE. FULL RANGE OF AIRFLOW.

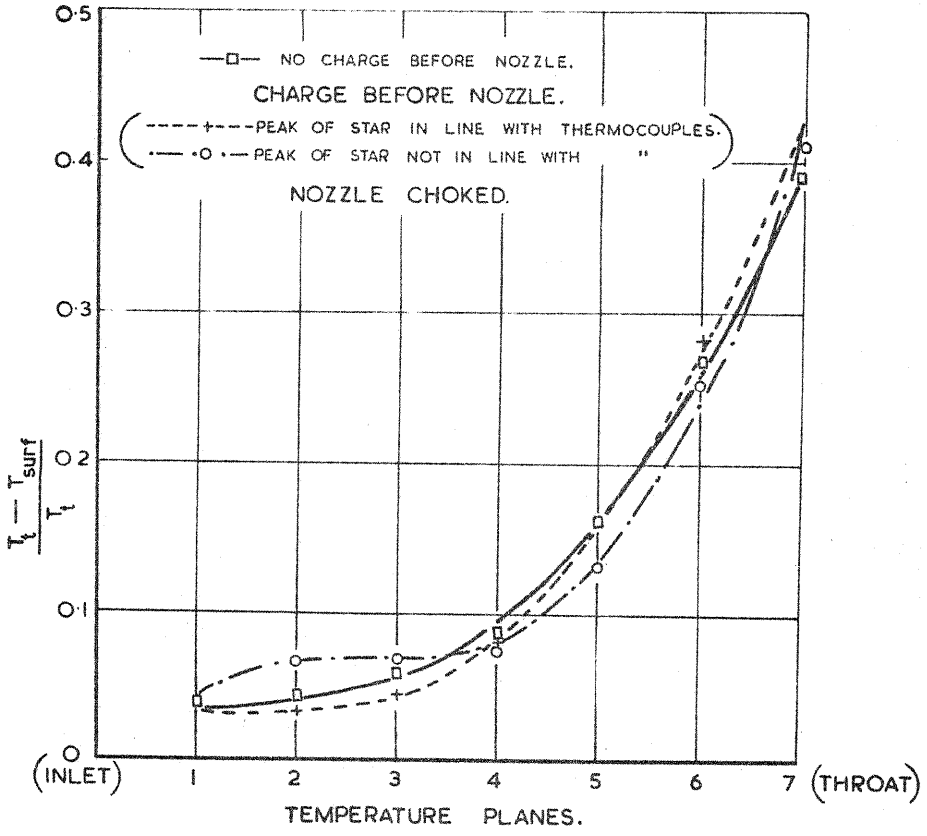

GRAPH. 4. VARIATION OF $\frac{T_t - T_{surf}}{T_t}$ ALONG NOZZLE SURFACE.

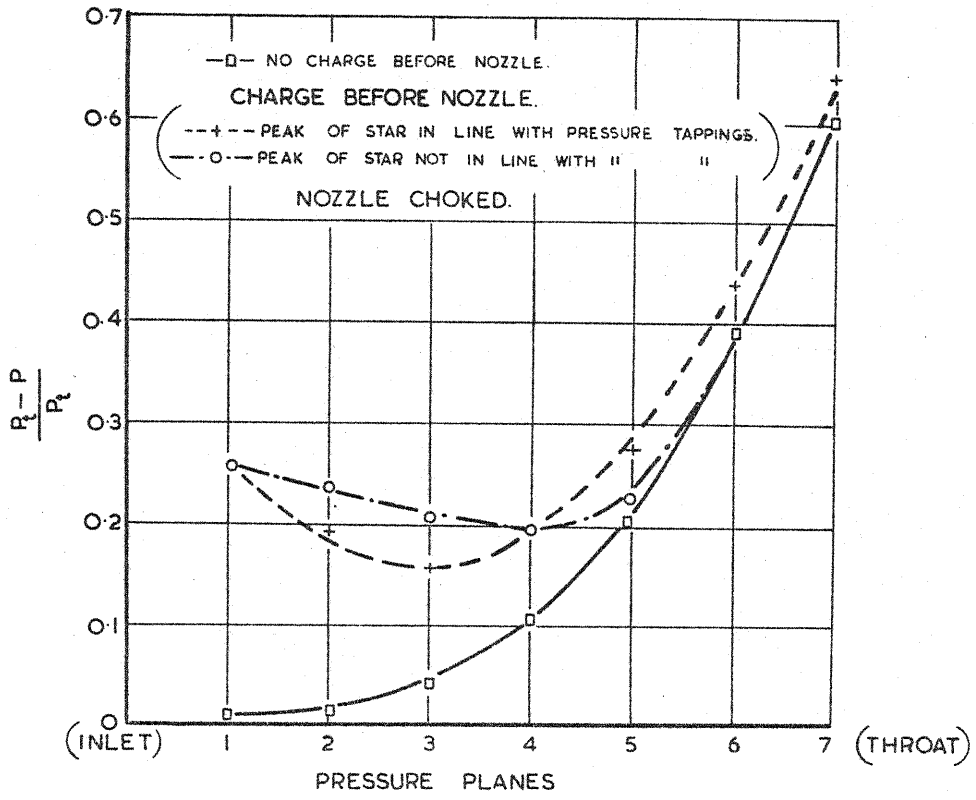

GRAPH. 5. VARIATION OF $\frac{P_t - P}{P_t}$ ALONG NOZZLE SURFACE.

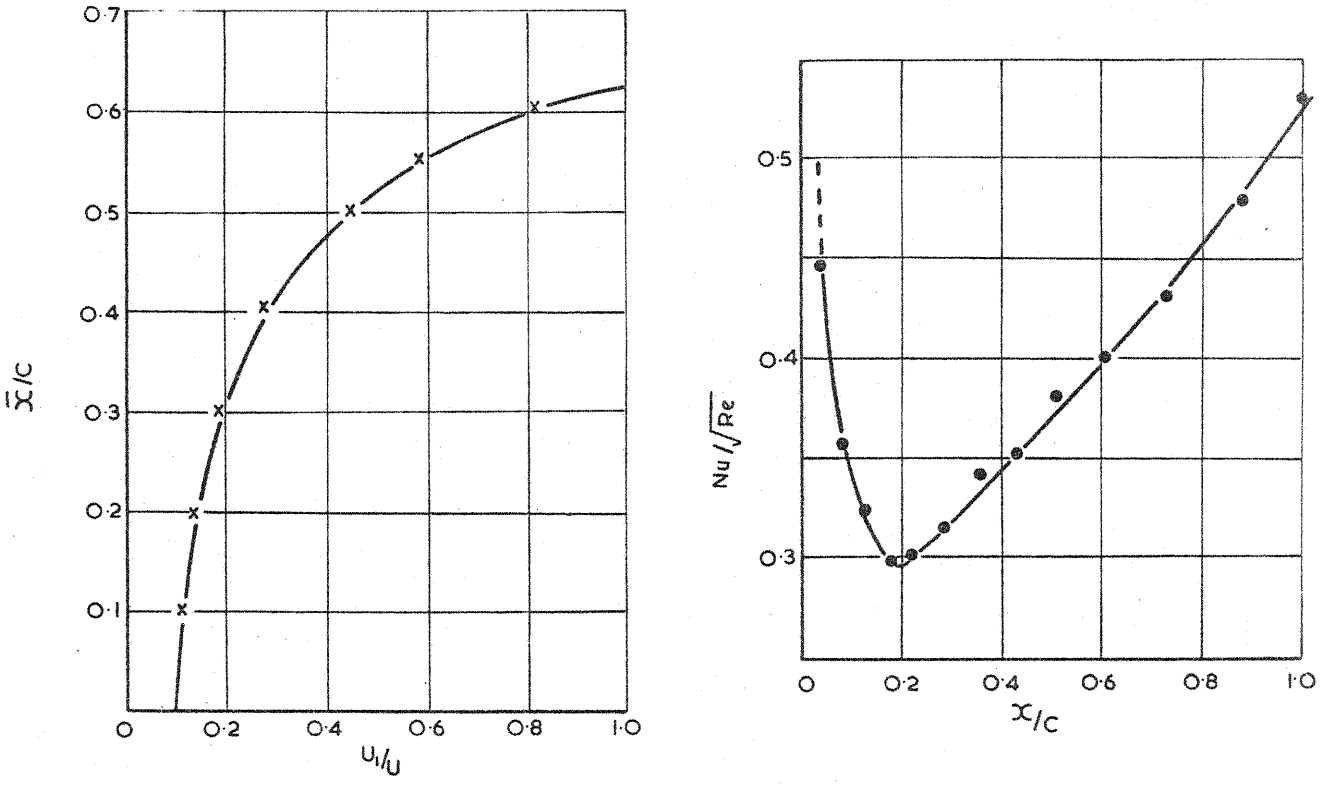

GRAPHS. 6.

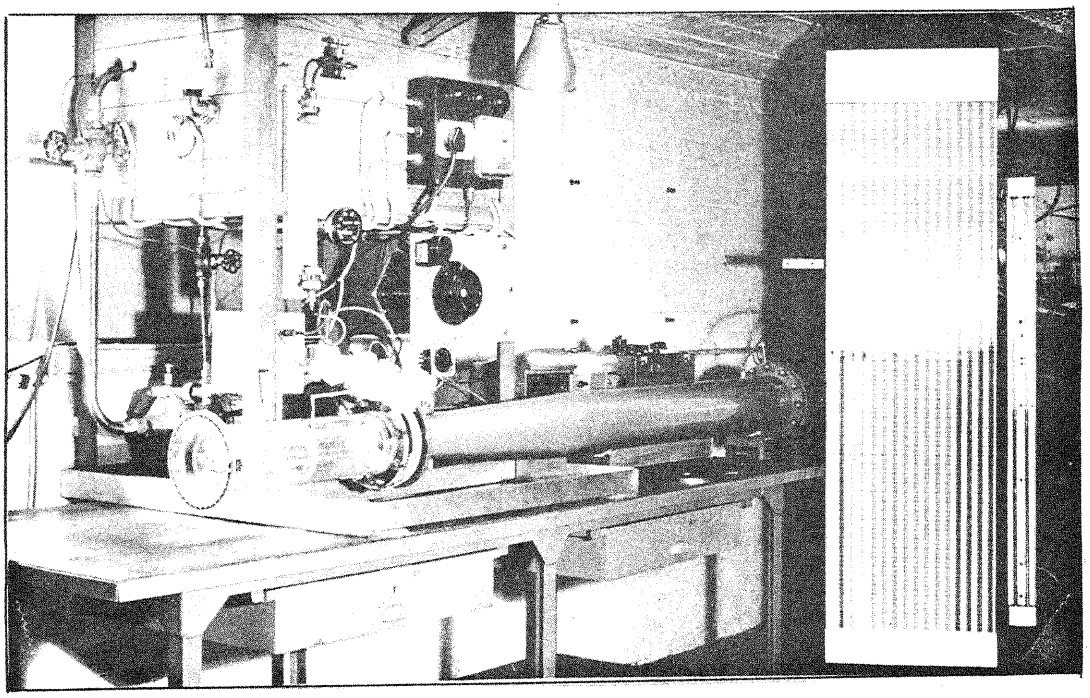

FIG. 1. HEAT TRANSFER RIG (CONSTANT FLOW CALORIMETRY)

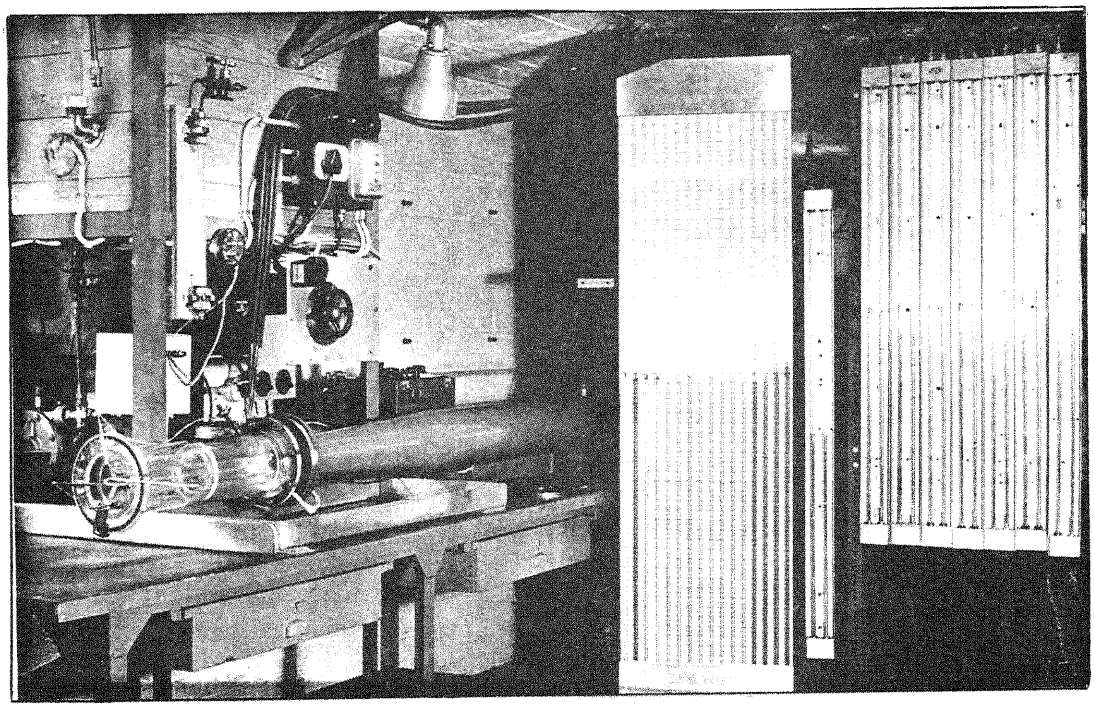

FIG. 2. RIG FOR DETERMINING THE ADIABATIC WALL TEMPERATURE DISTRIBUTION

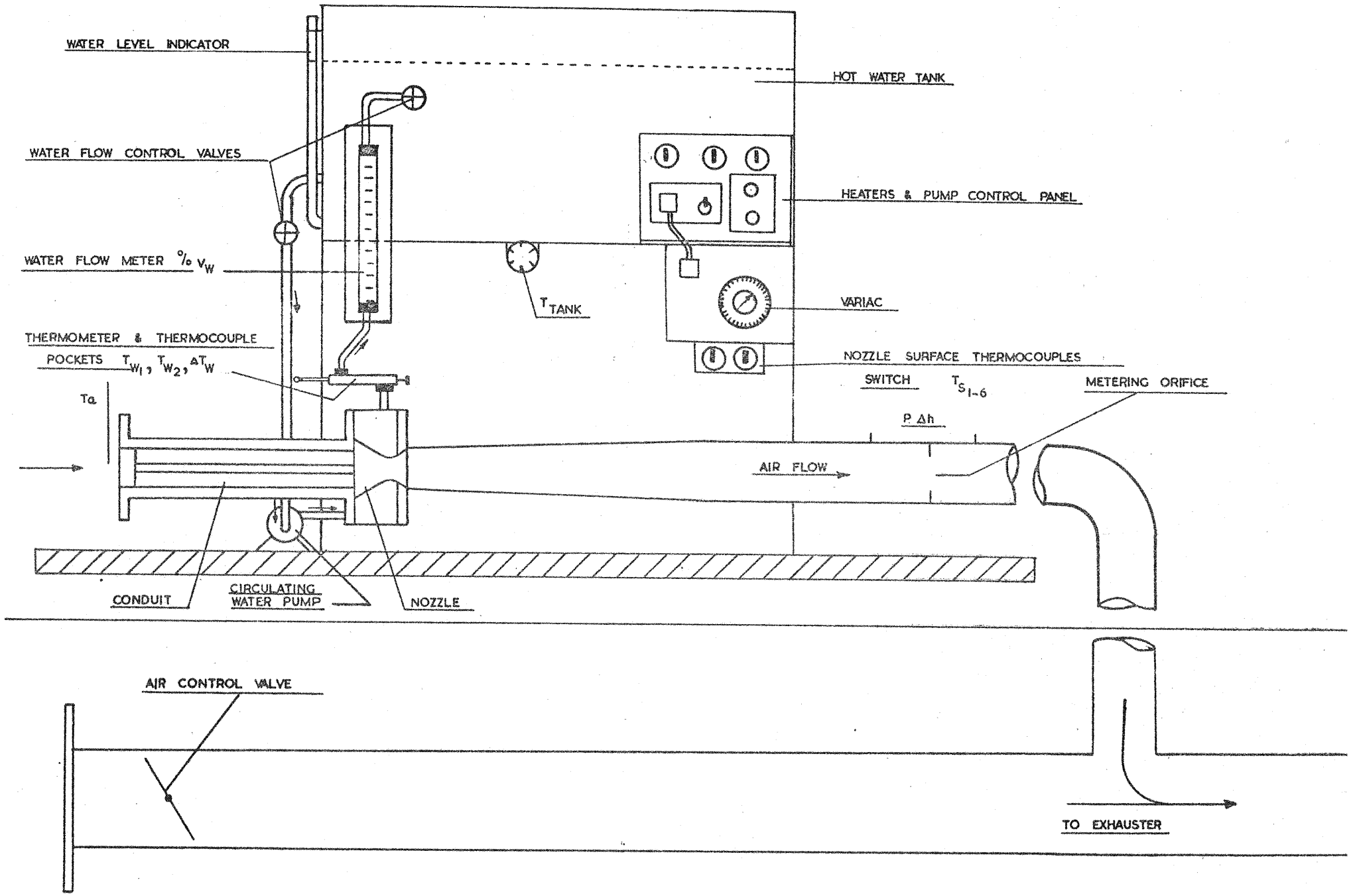

FIG. 3. DIAGRAMMATIC LAYOUT OF HEAT TRANSFER RIG.

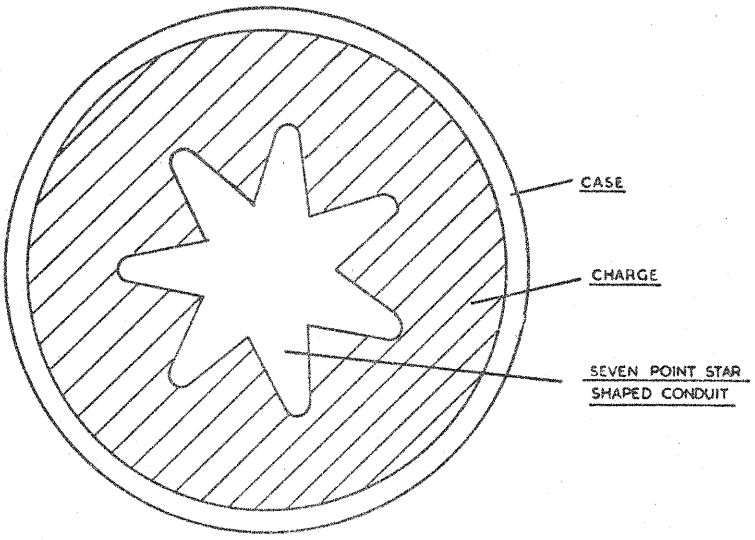

FIG. 4. CROSS SECTION OF CHARGE

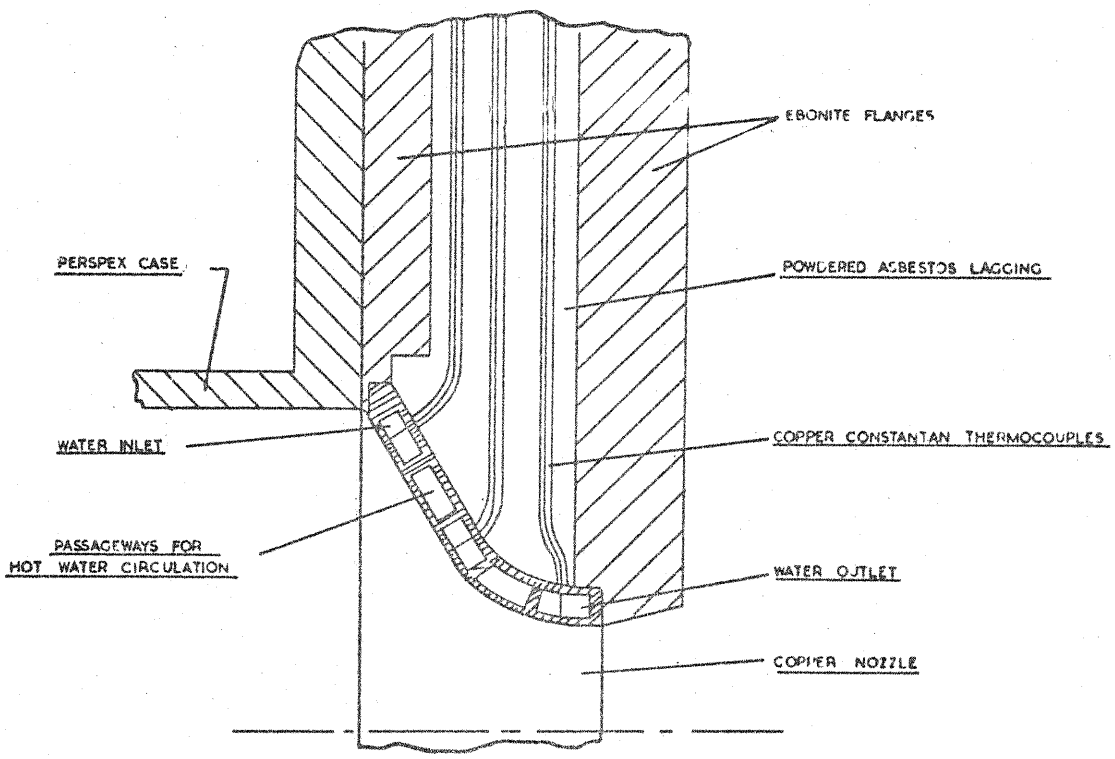

FIG. 5. SECTION OF COPPER NOZZLE

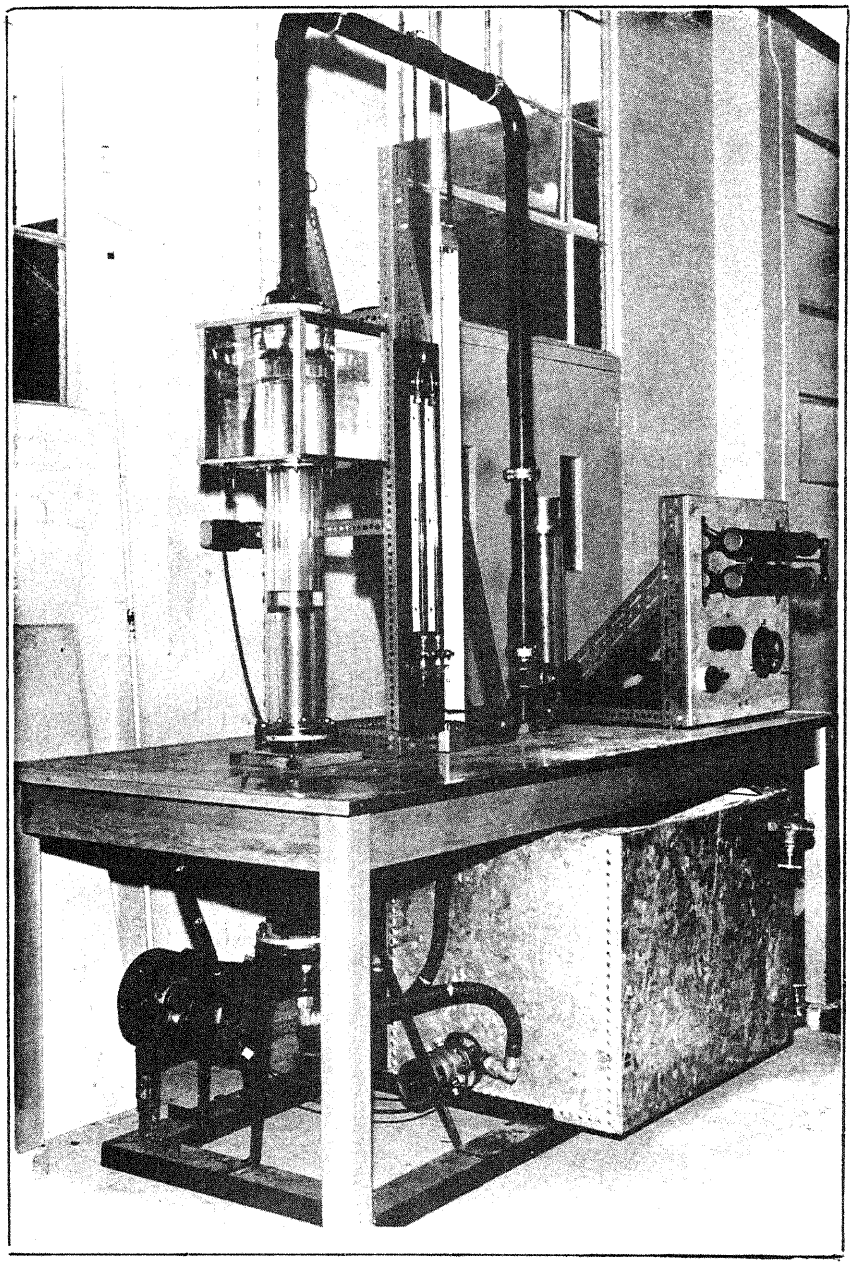

FIG. 6. FLOW VISUALISATION APPARATUS

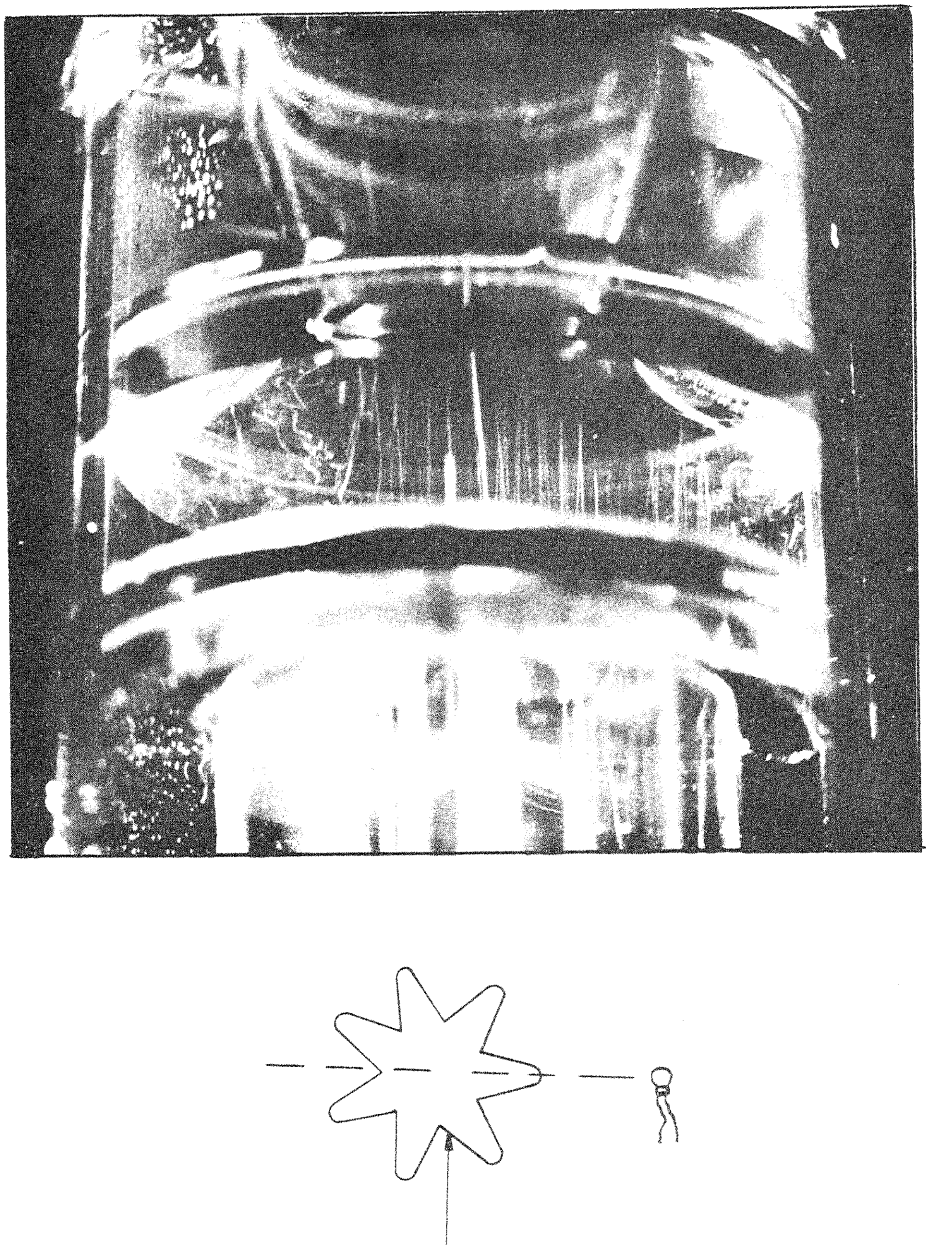

FIG. 7. FLOW VISUALISATION PHOTOGRAPH

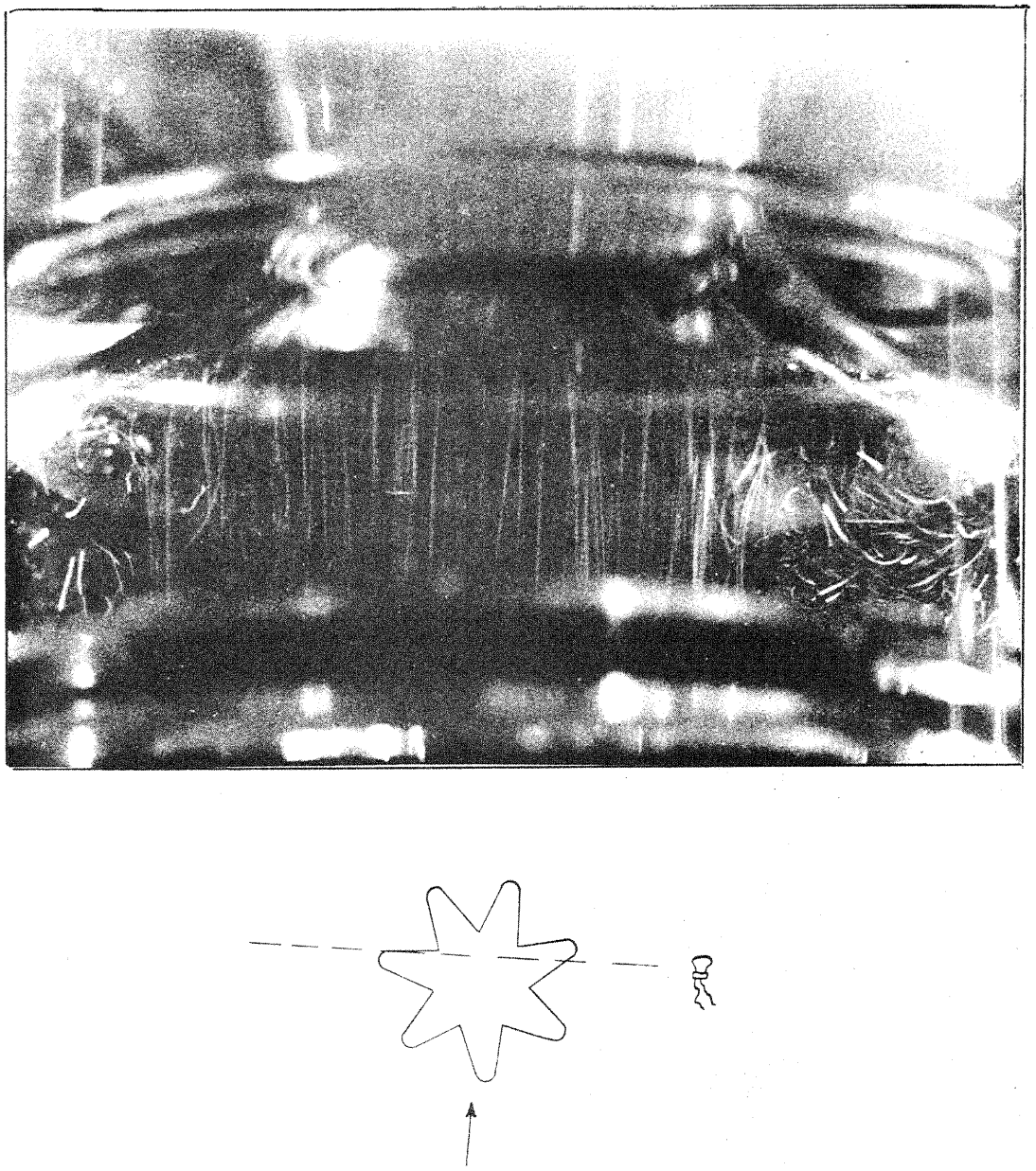

FIG. 8. FLOW VISUALISATION PHOTOGRAPH

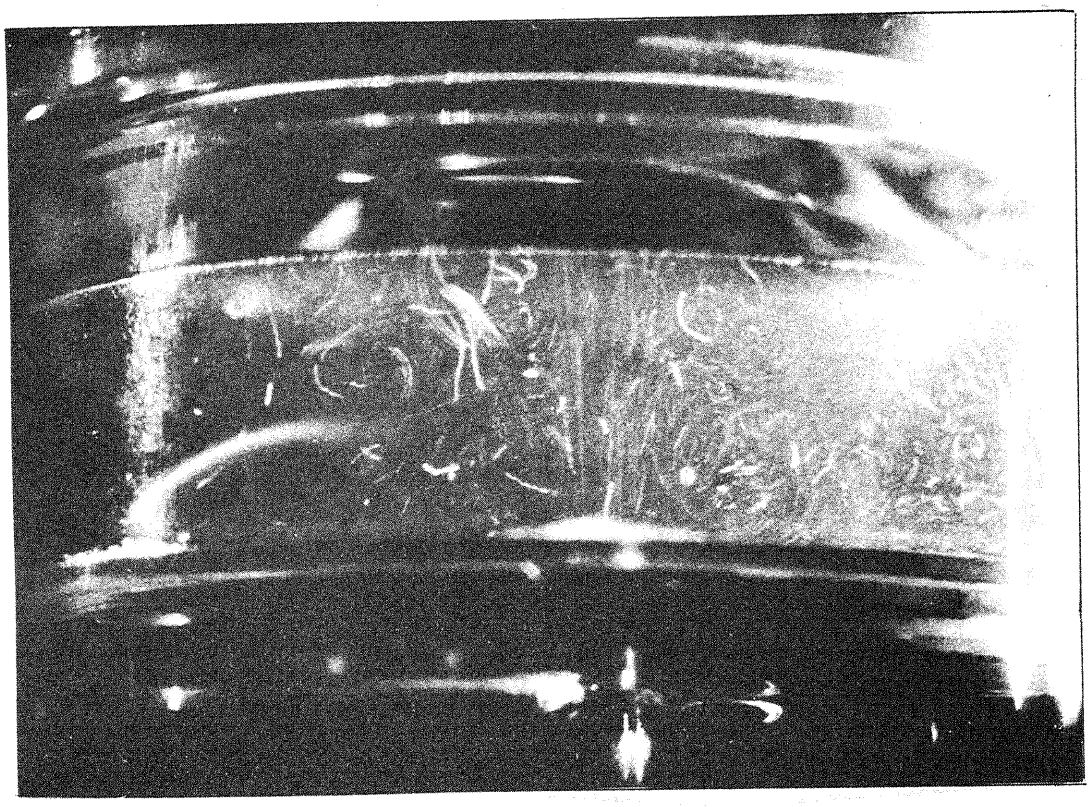

FIG. 9. FLOW VISUALISATION PHOTOGRAPH

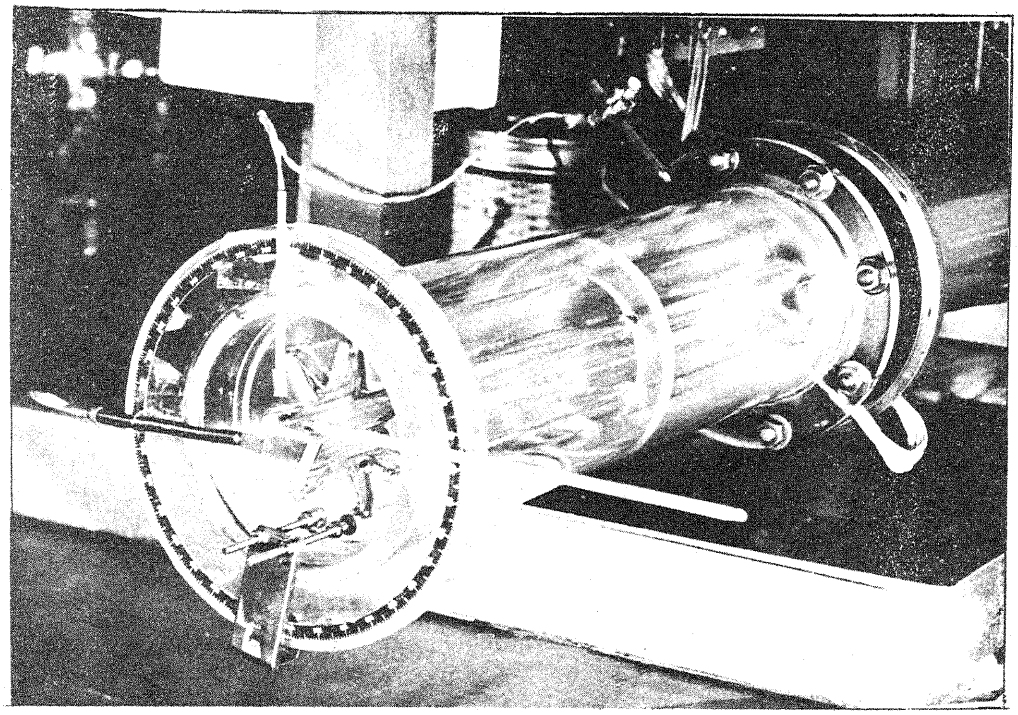

FIG. 10. PERSPEX CASING AND CONDUIT

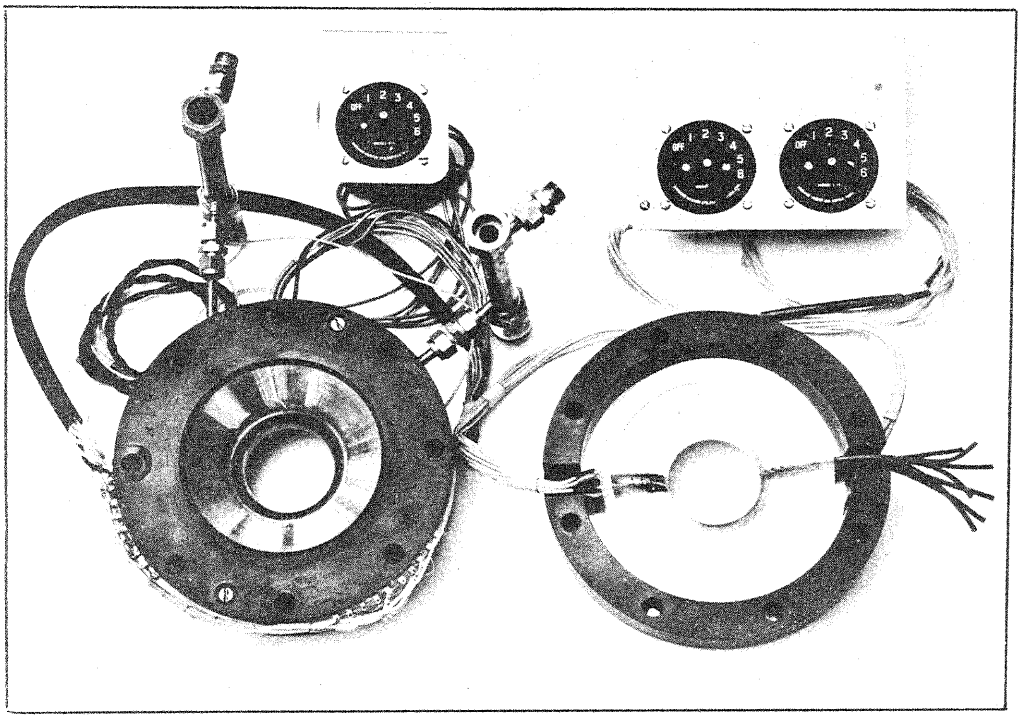

FIG. 11. COPPER NOZZLE AND PERSPEX NOZZLE